01 May 2022

Solid-State Formation Mechanisms of Core–shell Microstructures in (Zr,Ta)B2 Ceramics

Anna N. Dorner

Frédéric Monteverde

William Fahrenholtz
Missouri University of Science and Technology, billf@mst.edu

Gregory E. Hilmas
Missouri University of sScience and Technology, ghilmas@mst.edu

Recommended Citation

A. N. Dorner et al., "Solid-State Formation Mechanisms of Core–shell Microstructures in (Zr,Ta)B2 Ceramics," *Journal of the American Ceramic Society*, vol. 105, no. 5, pp. 3147 - 3152, Wiley, May 2022. The definitive version is available at https://doi.org/10.1111/jace.18363

Received: 24 October 2021 | Revised: 3 January 2022 | Accepted: 6 January 2022

DOI: 10.1111/jace.18363

Journal of the American Ceramic Society

RAPID COMMUNICATION

Solid-state formation mechanisms of core–shell microstructures in (Zr,Ta)B_2 ceramics

Anna N. Dorner[1] | **Frédéric Monteverde**[2] | **William G. Fahrenholtz**[1] | **Gregory E. Hilmas**[1]

[1] Department of Materials Science and Engineering, Missouri University of Science and Technology, Rolla, Missouri, USA

[2] CNR-ISTEC, National Research Council of Italy – Institute of Science and Technology for Ceramics, Faenza, Italy

Correspondence
Anna N. Dorner, Department of Materials Science and Engineering, Missouri University of Science and Technology, Rolla, MO 65409-0330, USA.
Email: andh2d@mst.edu

Funding information
Honeywell Federal Manufacturing and Technologies, Grant/Award Number: N000335755

Abstract

Transition metal diborides with core–shell microstructures have demonstrated excellent mechanical properties at elevated temperatures. Previous studies concluded that core–shell microstructures were formed by liquid-assisted mass transport mechanisms, but in this study, we propose a solid-state formation mechanism for core-shell microstructures in (Zr,Ta)B_2 ceramics produced by reaction hot pressing and in ZrB_2-TaB_2 diffusion couples. Diffusion couple experiments demonstrated that core–shell microstructures developed as a result of Ta diffusion along ZrB_2 grain boundaries, which occurred concurrently with lattice diffusion of Ta into ZrB_2. These findings suggest that with optimization of batching and processing parameters, core–shell diboride materials may be formed through solid-state processes rather than liquid-assisted processes, which could assist in raising the upper temperature limits of use for these materials.

KEYWORDS
core–shell microstructure, interdiffusion, solid solution, tantalum diboride, zirconium diboride

1 | INTRODUCTION

Zirconium diboride, an ultra-high temperature ceramic, is a candidate for applications in extreme environments due to desirable properties such as high melting temperature (~3250°C), high thermal conductivity (up to ~140 W/m·K at 298 K), and good oxidation resistance.[1,2] In addition, ZrB_2 ceramics are capable of retaining their mechanical properties well above the melting temperatures of other materials such as oxide ceramics and metal alloys. The highest values of strength above 1500°C have been reported for diboride ceramics with core–shell microstructures. Specifically, in 2017, Silvestroni et al. reported that a ZrB_2-WC-SiC ceramic demonstrated mean strengths of 840 MPa at 1800°C and 660 MPa at 2100°C, which were approximately double the highest values previously reported for ZrB_2 ceramics at the same temperatures.[3] Additional studies have also reported favorable properties for diborides with core–shell microstructures.[4–6] For example, the average flexural strengths reported for a core–shell (Zr,Ta)B2 ceramic were 598 MPa at 1200°C and 374 MPa at 1500°C,[4] compared to those of a ZrB2-TaB2 composite without core–shell microstructure, which had strengths of 401 MPa at 1000°C, 336 MPa at 1600°C, and 256 MPa at 1800°C.[7]

Under certain processing conditions, transition metal (TM) diborides containing a second dissolved TM can form core–shell microstructures that consist of a core of nominally pure diboride with an epitaxial shell that is composed of a solid solution diboride.[3,8–12] Several TMs including Hf, Ta, Nb, Mo, and W can substitute onto the metal sites in ZrB_2 to form substitutional solid solutions.[13] In core–shell microstructures, the solid solution shells can contain from 3 to 20 at% or more of the second TM.[3,8,9,14] Typically, these materials have been produced by hot pressing or spark plasma sintering of mixtures of a primary TM compound (e.g., ZrB_2) with a compound containing a second TM such

as Mo, Ta, or W. Most reported diborides with core–shell microstructures also contain a source of silicon, such as SiC or a TM disilicide.[10,15–17]

Formation of the core–shell microstructure has been attributed to a transient liquid phase that forms due to the reaction of Si with residual surface oxides.[8,18,19] However, some studies have demonstrated the formation of core–shell materials in systems that do not contain Si, such as TiB_2-WC and ZrB_2-W, although core–shell formation was still attributed to liquid phase processes.[20,21] Monteverde et al. studied Si-free core-shell formation in the $(Zr,Mo)B_2$ system by hot pressing ZrB_2 and Mo powders at 1927°C and 32 MPa for 60 min.[15] While the powder compact only achieved 75% relative density, $(Zr,Mo)B_2$ solid solution shells/necks had begun to form on the surfaces of ZrB_2 particles. Due to the low relative density, the authors theorized that complete densification of similar materials would require a transient liquid phase that could facilitate more rapid mass transport. In the same study, ZrB_2-Mo-ZrB_2 diffusion couples were prepared at 1927°C to probe for the formation of a core–shell microstructure along the interface. However, crystalline Mo-B phases such as MoB and Mo_2B formed preferentially instead of $(Zr,Mo)B_2$, which the authors attributed to insufficient Mo solubility into ZrB_2 as well as a lack of mass transport pathways.

The $(Zr,Ta)B_2$ system forms core–shell microstructures. This system has been studied previously based on the observation that Ta-containing compounds can improve the oxidation resistance of ZrB_2 ceramics at temperatures of up to 1650°C.[22–24] The purpose of the present research was to study the formation of core–shell microstructures in the ZrB_2-TaB_2 system.

2 | EXPERIMENTAL SECTION

A reactive hot-pressing process, described in a previous study, was used to prepare the ceramics in the present study.[25] The three compositions that were prepared were nominally phase-pure ZrB_2 and TaB_2, along with a ceramic with a target stoichiometry of $(Zr_{0.5}Ta_{0.5})B_2$, termed ZT50. The precursors were commercial ZrH_2 (95.5% min; CRS Chemicals, Canoga Park, CA), amorphous boron (SP-95; SB Boron Products, Bellwood, IL), and phenolic resin (GP 2074; Georgia Pacific, Atlanta, GA). In addition, Ta_2H was prepared from Ta using a process developed by Schwind et al.[26] Diffusion couples were prepared by polishing ZrB_2 and TaB_2 sections to a 0.25 μm surface finish using progressively finer diamond abrasives. Couples were assembled by placing polished sides together in a graphite clamp, which kept the assembly together during annealing. Diffusion couple heat treatments were carried out in a graphite element furnace (1000-4560-FP30; Thermal Technologies, Santa Rosa, CA) in a flowing He atmosphere. For all treatments, the samples were heated at 25°C/min to 1650°C before ramping at 50°C/min to the final temperature.

Portions of ZT50 were crushed with a zirconia mortar and pestle and sieved to −200 mesh for X-ray diffraction (XRD; X'Pert Pro, PANalytical, Almelo, The Netherlands). Diffraction patterns were obtained with a tube current of 40 mA, a generator voltage of 45 keV, and Cu-Kα radiation (λ = 1.54056 Å). Scans were collected between 5 and 138° 2θ with a step size of 0.026° 2θ and a total scan time of 1 h. Samples were prepared for scanning electron microscopy using the polishing procedure described above, with a final surface polish of 0.25 μm. Scanning electron microscopy (SEM; ZEISS Sigma, Carl Zeiss Sigma NTS GmbH, Oberkochen, Germany) of ZT50 was conducted with an accelerating voltage of 10 kV, a working distance of 7.5 mm, an aperture of 60 μm, and a backscattered electron (BSE) detector to enhance composition contrast. Energy-dispersive spectroscopy (EDS) maps of ZT50 sample were collected with an accelerating voltage of 20 kV, a working distance of 12.2 mm, an aperture of 60 μm, resolution of 610 × 457 px, a dwell time of 128 μs, and a frame count of approximately 5 (Quantax 200; Bruker, Billerica, MA). SEM (Quanta 600 FEG, FEI, Hillsboro, OR) and EDS (Quantax 200; Bruker) of diffusion couples were collected with an accelerating voltage of 25 kV, a working distance of 10 mm, an aperture of 100 μm, and a BSE detector. EDS maps were collected with a silicon drift detector with a 30 mm^2 active area by manual acquisition using a resolution of 1024 × 884 px, a pixel time of 8 μs, and a frame count of approximately 40.

3 | RESULTS AND DISCUSSION

The relative densities of the ceramics used in the diffusion couples were 98% for ZrB_2 and 96% for TaB_2. The ZT50 ceramic had a bulk density of 8.721 g/cm^3, a calculated theoretical density of 9.097 g/cm^3, and a resultant relative density of 95.9%. XRD analysis found that the as-sintered ZT50 ceramic contained three distinct sets of diboride peaks (Figure 1A). These three sets of diboride peaks corresponded to pure ZrB_2 and two $(Zr,Ta)B_2$ (shortened ZTB) solid solutions with different compositions. Dissolution of Ta into ZrB_2 decreases the lattice parameters due to the smaller atomic radius of Ta compared to Zr, which shifts the diffraction peaks to larger values of 2θ.[25,27] The combination of peaks for nominally pure ZrB_2 along with peaks for $(Zr,Ta)B_2$ solutions was a possible indication of core–shell formation, as peak splitting (i.e., peaks for the same structure with different lattice parameters) is characteristic of core–shell materials.[8,10,17] Microstructure analysis also revealed that three distinct phases were present

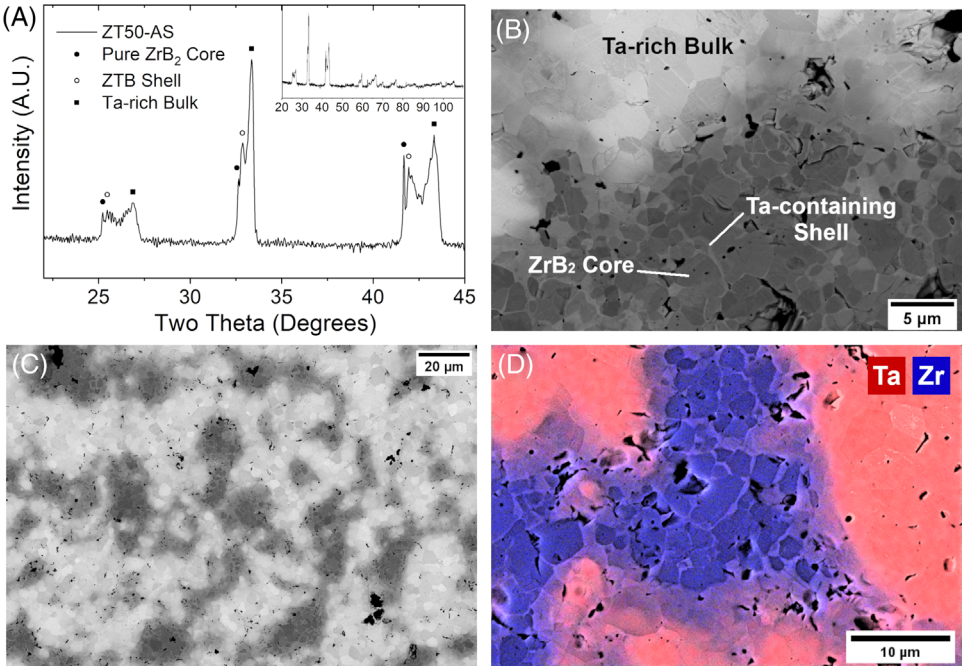

FIGURE 1 (A) X-ray diffraction (XRD) diffraction pattern, (B) annotated backscattered electron (BSE) micrograph, (C) bulk view BSE micrograph, and (D) energy-dispersive spectroscopy (EDS) mapping of core–shell-containing ZT50 material

in ZT50, and a core–shell microstructure was observed in the as-sintered ceramic (Figure 1B). The microstructure had regions that consisted of ZrB_2 cores and ZTB shells, which, in turn, were surrounded by a brighter-contrast, more Ta-rich solid solution bulk (Figure 1C). The compositions were confirmed with EDS mapping (Figure 1D). The formation of core–shell microstructures was not anticipated for these processing conditions because other single-phase ZTB solid solutions with lower Ta contents have been prepared by the same methodology.[25,27] Furthermore, no Si or other transient liquid-forming source was present in the batched precursors.

Diffusion couples of ZrB_2 and TaB_2 were used to investigate the formation of core–shell structures. Two diffusion couples were analyzed; one prepared at 2200°C for 12 h (DC 22-12) and one prepared at 2100°C for 8 h (DC 21–8). BSE micrographs and EDS maps are shown in Figure 2 with TaB_2 having brighter contrast than ZrB_2. From both compositional contrast in the micrographs and EDS mapping of Zr and Ta, an interfacial region of ZTB solid solution was formed by interdiffusion during the heat treatments. From the image, Zr diffusion into TaB_2 resulted in a uniform interface. In contrast, Ta diffusion into ZrB_2 occurred along ZrB_2 grain boundaries, which formed core–shell like regions, particularly in DC 22-12. These findings illuminated how the three-phase microstructure of ZT50 may have developed. Initially, pure ZrB_2 and either pure TaB_2 or a ZTB solid solution were formed. However, as interdiffusion between these species proceeded, Zr diffused into Ta-containing phases by lattice diffusion (i.e., a uniform diffusion front), while Ta was transported into ZrB_2 by grain boundary diffusion. Lattice diffusion of Ta into ZrB_2 also occurred in the diffusion couples, resulting in Ta-containing interdiffusion regions that were distinct from the core–shell regions. Despite heat treating DC 22-12 for longer at a higher temperature, compared to DC-21-8, lattice diffusion did not overtake grain boundary diffusion and, instead, evidence of both mechanisms is visible. Hence, the rates of grain boundary and lattice diffusion appear to be similar for Ta diffusion into ZrB_2.

Previously, Monteverde et al. proposed that the transport of Mo along ZrB_2 grain boundaries to form $(Zr,Mo)B_2$ core–shell materials was facilitated by open porosity and the presence of a transient liquid phase.[15] Neither of these were present in the diboride ceramics in the present study because the hot-pressed materials did not contain any Si, and the diffusion couples showed transport of Ta along ZrB_2 grain boundaries in dense ceramics without any open porosity. Core–shell microstructures are generally produced at temperatures at or below 1950°C with higher densification temperatures resulting in homogeneous $(Zr,TM)B_2$ solid solutions.[15] Lonergan et al. showed that the densification mechanism of ZrB_2 changed from grain boundary diffusion at lower temperatures to lattice diffusion at 2000°C.[28] If a similar change in the predominant mass transport mechanism occurs for the diffusion of other TMs in ZrB_2, core–shell microstructures do not require the presence of a liquid phase to assist mass transport

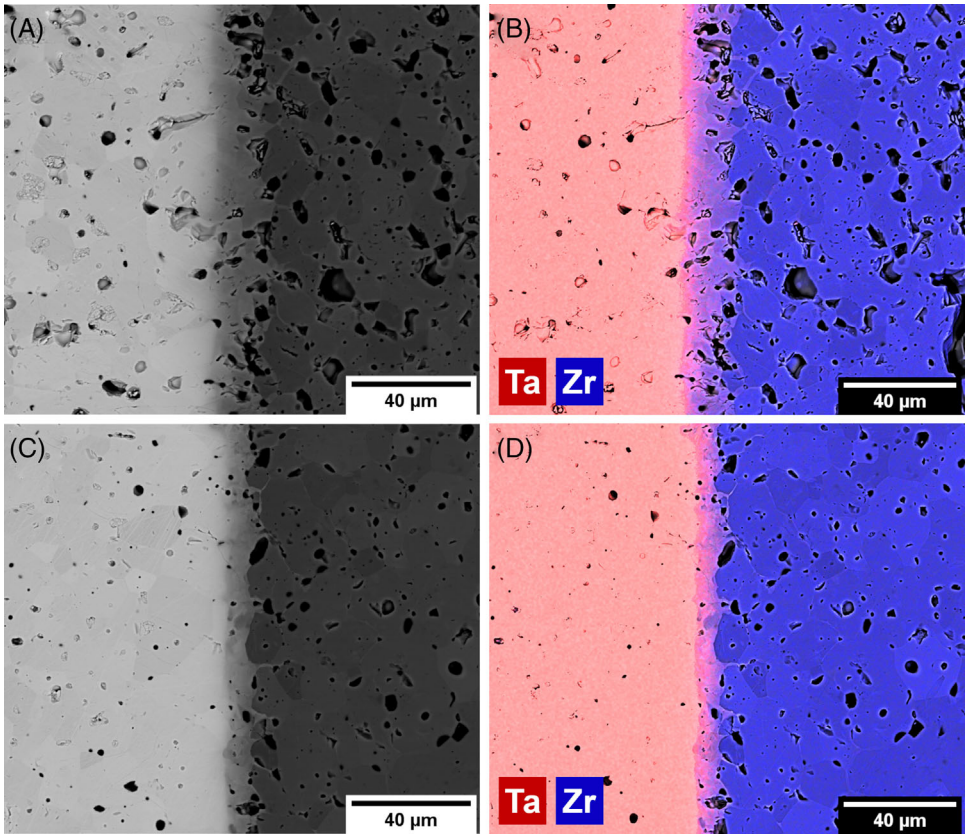

FIGURE 2 (A) Backscattered electron (BSE) micrograph and (B) energy-dispersive spectroscopy (EDS) mapping of DC 22-12 and (C) BSE micrograph and (D) EDS mapping of DC 21–8

along grain boundaries. All materials analyzed in the present study were prepared and annealed at temperatures above 2000°C, which would mean that lattice diffusion would be the predominant diffusion mechanism. However, grain boundary diffusion, which has a lower activation energy than lattice diffusion, is still active at these temperatures. In fact, other polycrystalline ceramic systems have been documented to exhibit concurrent interdiffusion by both lattice and grain boundary diffusion mechanisms.[29] Based on observations supported by SEM analysis and EDS mapping, we propose that Zr diffusion into the TaB_2 bulk occurs primarily through lattice diffusion, whereas Ta diffusion into the ZrB_2 bulk occurs through both lattice and grain boundary diffusion. Other TMs such as W and Mo that form similar core–shell microstructures in ZrB_2 likely also exhibit this type of behavior. Further, the formation of these structures can occur by solid-state mechanisms without the presence of a transient liquid phase or silicon. Instead, the formation of core–shell microstructures can occur due to a natural competition between grain boundary and lattice diffusion mechanisms.

These results constitute one of the first documented cases of core–shell formation in diborides as a result of solid-state interdiffusion processes rather than liquid-facilitated mass transport during densification. If other similar systems exhibit similar competitions between lattice and grain boundary diffusion mechanisms, then the formation of core–shell microstructures may be possible in other systems without the use of liquid-forming additives. The possible application temperatures for diboride materials can approach 3000°C—far beyond the temperature regimes explored so far in mechanical properties testing. As researchers push for higher temperature testing, the evolution of liquid phases in typical core–shell ceramics will present upper temperature limits for their use. However, these results indicate that solid-state production of core–shell ceramics may be feasible, which could extend the use of diborides with core–shell microstructures to higher temperatures. Even with liquid-forming additives, current core–shell diboride ceramics demonstrate superior elevated temperature mechanical properties over other diboride ceramics, and so core–shell ceramics devoid of these additives may continue to deliver excellent mechanical properties, which extend into temperature regimes beyond those which additive-containing diboride ceramics can withstand.

4 | CONCLUSIONS

Core–shell microstructures were observed in (Zr,Ta)B_2 ceramics produced by reactive hot pressing as well as in the interfacial regions of ZrB_2-TaB_2 diffusion couples. Although previous studies of core–shell microstructures in diborides attributed formation to mass transport by a transient liquid phase and open porosity, neither liquid phases nor open porosity was observed in the (Zr,Ta)B_2 ceramics in the present study. Diffusion couple experiments demonstrated that the (Zr,Ta)B_2 core–shell microstructures developed as a result of solid-state Ta interdiffusion along ZrB_2 grain boundaries, which occurred concurrently with lattice diffusion. These results demonstrate core–shell diboride production without the use of liquid-forming or silicon-containing additives, which is a promising route for the development of refractory diboride ceramics with superior elevated temperature mechanical properties.

ACKNOWLEDGMENTS

This work was funded by Honeywell Federal Manufacturing and Technologies through contract number N000335755. Honeywell Federal Manufacturing & Technologies, LLC operates the Kansas City National Security Campus for the United States Department of Energy/National Nuclear Security Administration under Contract Number DE-NA0002839. The authors thank Dr. Tieshu Huang for his technical guidance and support. The authors would also like to thank Dr. Jeremy Watts, Dr. Clarissa Wisner, Dr. Eric Bohannan, and the Advanced Materials Characterization Laboratory at Missouri S&T for their assistance with sample preparation and characterization, and Dr. David Stalla and the University of Missouri Electron Microscopy Core for their assistance with SEM/EDS.

ORCID

Anna N. Dorner https://orcid.org/0000-0001-8971-1199
Frédéric Monteverde https://orcid.org/0000-0002-9766-2275
William G. Fahrenholtz https://orcid.org/0000-0002-8497-0092

REFERENCES

1. Fahrenholtz WG, Hilmas GE, Talmy IG, Zaykoski JA. Refractory diborides of zirconium and hafnium. J Am Ceram Soc. 2007;90(5):1347-64.
2. Stanfield AD, Fahrenholtz WG, Hilmas GE. Effects of Ti, Y, and Hf additions on the thermal properties of ZrB_2. J Eur Ceram Soc. 2020;40(12):3824-8.
3. Silvestroni L, Kleebe H-J, Fahrenholtz WG, Watts J. Super-strong materials for temperatures exceeding 2000 °C. Sci Rep. 2017;7:40730.
4. Sciti D, Silvestroni L, Celotti G, Melandri C, Guicciardi S. Sintering and mechanical properties of ZrB_2–$TaSi_2$ and HfB_2–$TaSi_2$ ceramic composites. J Am Ceram Soc. 2008;91(10):3285-91.
5. Grohsmeyer RJ, Silvestroni L, Hilmas GE, Monteverde F, Fahrenholtz WG, D'Angió A, et al. ZrB_2-$MoSi_2$ ceramics: a comprehensive overview of microstructure and properties relationships. Part II: mechanical properties. J Eur Ceram Soc. 2019;39(6):1948-54.
6. Monteverde F, Melandri C, Failla S, Grohsmeyer RJ, Hilmas GE, Fahrenholtz WG. Escape from the strength-to-toughness paradox: bulk ceramics through dual composite architectures. J Eur Ceram Soc. 2018;38(8):2961-70.
7. Demirskyi D, Vasylkiv O. Flexural strength behavior of a ZrB_2–TaB_2 composite consolidated by non-reactive spark plasma sintering at 2300°C. Int J Refract Met Hard Mater. 2017;66:31-5.
8. Silvestroni L, Sciti D. Densification of ZrB_2–$TaSi_2$ and HfB_2–$TaSi_2$ ultra-high-temperature ceramic composites. J Am Ceram Soc. 2011;94(6):1920-30.
9. Silvestroni L, Gilli N, Migliori A, Sciti D, Watts J, Hilmas GE, et al. A simple route to fabricate strong boride hierarchical composites for use at ultra-high temperature. Compos Part B Eng. 2020;183:107618.
10. Hu C, Sakka Y, Gao J, Tanaka H, Grasso S. Microstructure characterization of ZrB_2–SiC composite fabricated by spark plasma sintering with $TaSi_2$ additive. J Eur Ceram Soc. 2012;32(7):1441-6.
11. Talmy IG, Zaykoski JA, Opeka MM. High-temperature chemistry and oxidation of ZrB_2 ceramics containing SiC, Si_3N_4, Ta_5Si_3, and $TaSi_2$. J Am Ceram Soc. 2008;91(7):2250-7.
12. Silvestroni L, Sciti D, Monteverde F, Stricker K, Kleebe H-J. Microstructure evolution of a W-doped ZrB_2 ceramic upon high-temperature oxidation. J Am Ceram Soc. 2017;100(4):1760-72.
13. Voroshilov YV, Kuz'ma YB. Reaction of zirconium with the transition metals and boron. Powder Metall Metal Ceram. 1969;8(11):941-4.
14. Silvestroni L, Kleebe H-J. Critical oxidation behavior of Ta-containing ZrB_2 composites in the 1500–1650°C temperature range. J Eur Ceram Soc. 2017;37(5):1899-908.
15. Monteverde F, Grohsmeyer RJ, Stanfield AD, Hilmas GE, Fahrenholtz WG. Densification behavior of ZrB_2-$MoSi_2$ ceramics: the formation and evolution of core-shell solid solution structures. J Alloys Compd. 2019;779:950-61.
16. Neuman EW, Brown-Shaklee HJ, Hilmas GE, Fahrenholtz WG. Titanium diboride–silicon carbide–boron carbide ceramics with super-high hardness and strength. J Am Ceram Soc. 2018;101(2):497-501.
17. Hu D-L, Gu H, Zou J, Zheng Q, Zhang G-J. Core–Rim structures and hierarchical phase relationship for hot-pressed ZrB 2–SiC–MC (M = Nb, Hf, Ta, W) ceramics. *SSRN*. 2019. https://doi.org/10.2139/ssrn.3358890
18. Silvestroni L, Kleebe H-J, Lauterbach S, Müller M, Sciti D. Transmission electron microscopy on Zr- and Hf-borides with $MoSi_2$ addition: densification mechanisms. J Mater Res. 2010;25(5):828-34.
19. Monteverde F. The addition of SiC particles into a $MoSi_2$-doped ZrB_2 matrix: effects on densification, microstructure and thermo-physical properties. Mater Chem Phys. 2009;113(2):626-33.
20. Chao S, Goldsmith J, Banerjee D. Titanium diboride composite with improved sintering characteristics. Int J Refract Met Hard Mater. 2015;49:314-9.

21. Ding H-J, Wang X-G, Xia J-F, Bao W-C, Zhang G-J, Zhang C, et al. Effect of solid solution and boron vacancy on the microstructural evolution and high temperature strength of W-doped ZrB_2 ceramics. J Alloys Compd. 2020;827:154293.
22. Levine SR, Opila EJ. Tantalum addition to zirconium diboride for improved oxidation resistance. 2003. NASA/TM–2003–212483.
23. Opila E, Levine S, Lorincz J. Oxidation of ZrB 2-and HfB 2-based ultra-high temperature ceramics: effect of Ta additions. J Mater Sci. 2004;39(19):5969-77.
24. Thimmappa SK, Golla BR. Effect of tantalum addition on microstructure and oxidation of spark plasma sintered ZrB_2-20vol% SiC composites. Ceram Int. 2019;45(11):13799-808.
25. Dorner AN, Barton DJ, Zhou Y, Thompson GB, Hilmas GE, Fahrenholtz WG. Solute distributions in tantalum-containing zirconium diboride ceramics. J Am Ceram Soc. 2020;103(4):2880-90.
26. Schwind EC, Hilmas GE, Fahrenholtz WG. Thermal properties and elastic constants of ζ-Ta4C3− x. J Am Ceram Soc. 2020;103(5):2986-90.
27. Dorner AN, Werbach K, Hilmas GE, Fahrenholtz WG. Effect of tantalum solid solution additions on the mechanical behavior of ZrB_2. J Eur Ceram Soc. 2021;41(6):3219-26.
28. Lonergan JM, Fahrenholtz WG, Hilmas GE. Sintering mechanisms and kinetics for reaction hot-pressed ZrB_2. J Am Ceram Soc. 2015;98(8):2344-51.
29. Paul A. Estimation of diffusion coefficients in binary and pseudo-binary bulk diffusion couples. In: Paul A, Divinski S, editors. Handbook of solid state diffusion. Volume 1. Amsterdam: Elsevier; 2017. p. 79–201.

How to cite this article: Dorner AN, Monteverde F, Fahrenholtz WG, Hilmas GE. Solid-state formation mechanisms of core–shell microstructures in $(Zr,Ta)B_2$ ceramics. J Am Ceram Soc. 2022;105:3147–3152.
https://doi.org/10.1111/jace.18363